

Energy Relaxation in Fermi-Pasta-Ulam Arrays

R. Reigada

Departament de Química Física

Universitat de Barcelona

Avda. Diagonal 647, 08028 Barcelona, Spain

A. Sarmiento

Instituto de Matemáticas

Universidad Nacional Autónoma de México

Ave. Universidad s/n, 62200 Chamilpa Morelos, México

Katja Lindenberg

Department of Chemistry and Biochemistry and

Institute for Nonlinear Science

University of California, San Diego, La Jolla, California 92093

November 21, 2018

Abstract

The dynamics of energy relaxation in thermalized one- and two-dimensional arrays with nonlinear interactions depend in detail on the interactions and, in some cases, on dimensionality. We describe and explain these differences for arrays of the Fermi-Pasta-Ulam type. In particular, we focus on the roles of harmonic contributions to the interactions and of breathers in the relaxation process.

PACS number(s): 05.40.-a, 05.45.-a, 63.20.Pw

1 Introduction

The ability of extended systems to support the localization and transport of vibrational energy has been invoked in a number of physical settings including DNA molecules [1], hydrocarbon structures [2], energy storage and transport in proteins [3, 4, 5], the creation of vibrational intrinsic localized modes in anharmonic crystals using an optimally chosen sequence of femtosecond laser pulses [6], photonic crystal waveguides [7], and targeted energy transfer between donors and acceptors in biomolecules [8]. It has become increasingly clear that thermal fluctuations may strongly affect (sometimes leading to degradation but at times actually helping) the process of energy localization and energy mobility [1, 2, 9, 10, 11, 12, 13, 14, 15, 16, 17]. It is thus clearly important to investigate the nature and dynamics of thermal fluctuations in nonlinear arrays. The understanding of the spatial and temporal evolution of the thermal relaxation landscape will in turn lead to a better understanding of other chemical and physical processes that may be occurring in the relaxing landscape.

The spatial and temporal evolution of an influx of energy into or an efflux of energy out of a nonlinear array, and the dynamical pathways that characterize energy relaxation in such an array, depend on a large number of factors (for recent reviews of a huge literature see [18, 19]). The nature of the interactions and where the nonlinearities reside (in the local potentials or in the interactions), the boundary conditions (free, fixed, or periodic), the size of the system, its dimensionality, the way in which energy is deposited in the system (initial conditions), etc., can all influence the evolution profoundly, and no general formalism that encompasses all these variations has yet been developed. It is thus necessary in this study (as in most others) to circumscribe the range of our inquiry. We have been particularly interested in discrete extended systems in which localized energy can also be *mobile* [11, 13, 14], and so our studies have focused on arrays with hard nonlinear interactions and no local potentials, specifically on Fermi-Pasta-Ulam (FPU) lattices. Some movement of localized energy may also occur in arrays with soft local potentials (see e.g. [1]), but it is much more difficult to achieve. We thus concentrate on FPU arrays.

Specifically in this paper we study energy relaxation in one-dimensional [20] and two-dimensional FPU arrays with quartic potentials. The Hamiltonian

in one dimension is

$$H = \sum_{i=1}^N \frac{\dot{x}_i^2}{2} + \frac{k}{2} \sum_{i=1}^N (x_i - x_{i-1})^2 + \frac{k'}{4} \sum_{i=1}^N (x_i - x_{i-1})^4 \quad (1)$$

where N is the number of sites; k and k' are the harmonic and anharmonic force constants, respectively. In two dimensions for an $N \times N$ lattice

$$H = \sum_{i,j=1}^N \frac{\dot{x}_{i,j}^2}{2} + \frac{k}{2} \sum_{i,j=1}^N [(x_{i,j} - x_{i-1,j})^2 + (x_{i,j} - x_{i,j-1})^2] + \frac{k'}{4} \sum_{i,j=1}^N [(x_{i,j} - x_{i-1,j})^4 + (x_{i,j} - x_{i,j-1})^4]. \quad (2)$$

To study energy relaxation we initially thermalize the system at temperature T (see below), then connect the boundary sites (two end sites for a 1d system, $4(N - 1)$ edge sites for 2d arrays) to a zero-temperature reservoir via damping terms, and observe the thermal relaxation of the array toward zero temperature [10, 20, 21, 22]. We find that relaxation occurs through an interesting cascade of decay times that is sensitively dependent on the precise form of the interactions. This leads us to focus on two issues in the relaxation process: 1) the explicit role of the harmonic terms vs. anharmonic terms in the FPU Hamiltonian, and 2) the effects of array dimensionality.

To thermalize the system to a given temperature T we augment the equations of motion resulting from Eqs. (1) with the Langevin prescription connecting each site to a heat bath. In one dimension

$$\ddot{x}_i = -\frac{\partial}{\partial x_i} [V(x_i - x_{i-1}) + V(x_{i+1} - x_i)] - \gamma_0 \dot{x}_i + \eta_i(t). \quad (3)$$

Here $V(x_i - x_j)$ is the FPU potential, γ_0 is the dissipation parameter, and the $\eta_i(t)$ are mutually uncorrelated zero-centered Gaussian δ -correlated fluctuations that satisfy the fluctuation-dissipation relation at temperature T :

$$\langle \eta_i(t) \rangle = 0, \quad \langle \eta_i(t) \eta_j(t') \rangle = 2\gamma_0 k_B T \delta_{ij} \delta(t - t'). \quad (4)$$

The brackets here and below denote an ensemble average, and k_B is Boltzmann's constant. The generalization to two dimensions is immediate. We implement free-end boundary conditions, that is, $x_0 = x_1$ and $x_N = x_{N+1}$ in

one dimension and $x_{0,j} = x_{1,j}$, $x_{N,j} = x_{N+1,j}$, $x_{i,0} = x_{i,1}$, and $x_{i,N} = x_{i,N+1}$ in two dimensions. For the integrations of the equations of motion we use the fourth order Runge-Kutta method.

The thermalization process involves the spontaneous emergence of anharmonic (including localized) modes. In order to understand the dynamics of such modes, we begin again with a thermalized array and explicitly inject a breather-like excitation of energy much higher than the thermal energy. We then observe how the entire system, thermalized array plus injected excitation, evolves and relaxes toward zero temperature.

In Sec. 2 we itemize the measures used to display the relaxation process. In Sec. 3 we present our relaxation results, obtained primarily from numerical simulations. Section 4 shows what happens to an explicitly injected local excitation as the arrays relax to zero temperature. Section 5 provides a brief summary and synthesis of the outcomes.

2 Measures of Thermal Relaxation

Once our system is thermalized to temperature T we disconnect it from the thermal bath (i.e., we remove the $\eta_i(t)$ and $\gamma_0 \dot{x}_i$ terms from Eq. (3) or the equivalent terms from the two-dimensional set of equations), and we connect the edge sites to a cold $T = 0$ reservoir through the addition of dissipative terms $-\gamma \dot{x}$ to the equations of motion for these sites. We then continue the integration using the thermalized positions and displacements as the initial conditions. An ensemble is constructed by repeating this experiment for different thermalized initial conditions. There are of course a variety of ways to display the outcome, and in our work we have chosen three. One, the most “global” measure, is to follow the decay of the total array energy $E(t)$ as a function of time. The second is to follow the spectrum of the system as a function of time. This gives a frequency-by-frequency picture of the relaxation process and therefore a more complete description. The third is to show a spatial energy landscape as a function of time.

The total energy $E(t)$ of the array is simply the Hamiltonian function evaluated with the displacements and velocities obtained from the equations of motion. For a one-dimensional *harmonic* array this function has been

calculated analytically by Piazza et al. [10] for small γ and large N :

$$\begin{aligned} \frac{E(t)}{E(0)} &= \frac{1}{\pi} \int_0^\pi dq e^{-2t/\tau(q)} = e^{-t/\tau_0} I_0(t/\tau_0) \\ &= \begin{cases} e^{-t/\tau_0} & \text{for } t \ll \tau_0, \\ \left(\frac{2\pi t}{\tau_0}\right)^{-1/2} & \text{for } t \gg \tau_0. \end{cases} \end{aligned} \quad (5)$$

In the first line I_0 is the modified zero-order Bessel function, and $\tau_0 = N/2\gamma$. The decay time $\tau(q)$ for phonons of wavevector q is

$$\frac{1}{\tau(q)} = \frac{1}{\tau_0} \cos^2\left(\frac{q}{2}\right). \quad (6)$$

The second line in Eq. (5) gives the short-time and long-time behaviors. The former is a simple exponential decay associated with the lowest frequency phonon mode since it has the shortest decay time. The power law relaxation arises from the cascade of different decay times of the different phonon modes. For finite N the decay becomes exponential again when only the modes near the band-edge of the spectrum still survive. Note that the decay is not exponential throughout (a common misapprehension for harmonic systems), although the initial exponential behavior does last longer the larger the system. Each phonon mode decays separately (exponentially) and independently of all the others. This translates to an independent and separate decay of each frequency portion of the spectrum (see below). The calculation of the total energy is more cumbersome but basically similar for two-dimensional arrays. One finds that the decay time for phonons of wavevector $\mathbf{q} = (q_x, q_y)$ is

$$\frac{1}{\tau(\mathbf{q})} = \frac{1}{\tau_0} \left[\cos^2\left(\frac{q_x}{2}\right) + \cos^2\left(\frac{q_y}{2}\right) \right], \quad (7)$$

which upon integration over wavevectors leads to

$$\frac{E(t)}{E(0)} = e^{-2t/\tau_0} I_0^2(t/\tau_0) = \begin{cases} e^{-2t/\tau_0} & \text{for } t \ll \tau_0, \\ \left(\frac{2\pi t}{\tau_0}\right)^{-1} & \text{for } t \gg \tau_0. \end{cases} \quad (8)$$

The behavior of $E(t)/E(0)$ for 1d and 2d *anharmonic* arrays is expected to be different than Eqs. (5) and (8), respectively. These behaviors will be presented in the next section.

Our second measure of thermal relaxation focuses on the decay pathways of the different spectral regions as the array cools down. We concentrate on the time evolution of the Fourier transform of the relative displacement correlation function. Relative displacements provide a particularly sensitive measure of how adjacent masses are moving relative to one another. In a thermalized array the spectrum of interest is defined as

$$S(\omega) = 2 \int_0^\infty d\tau C(\tau) \cos \omega\tau, \quad (9)$$

where in one dimension

$$C(\tau) = \frac{1}{(N-1)} \sum_{i=2}^N \langle \delta_i x_i(t+\tau) \delta_i x_i(t) \rangle \quad (10)$$

and $\delta_i x_i(t)$ is the relative displacement

$$\delta_i x_i(t) \equiv x_i(t) - x_{i-1}(t). \quad (11)$$

In two dimensions

$$\begin{aligned} C(\tau) &= \frac{1}{N(N-1)} \sum_{i=2}^N \sum_{j=1}^N \langle \delta_i x_{i,j}(t+\tau) \delta_i x_{i,j}(t) \rangle \\ &+ \frac{1}{N(N-1)} \sum_{i=1}^N \sum_{j=2}^N \langle \delta_j x_{i,j}(t+\tau) \delta_j x_{i,j}(t) \rangle \end{aligned} \quad (12)$$

where

$$\delta_i x_{i,j}(t) \equiv x_{i,j}(t) - x_{i-1,j}(t), \quad \delta_j x_{i,j}(t) \equiv x_{i,j}(t) - x_{i,j-1}(t). \quad (13)$$

The thermal equilibrium spectrum for harmonic arrays in one [14] and two dimensions can be calculated analytically. In one dimension with periodic boundary conditions (for sufficiently long chains the boundary conditions do not affect the equilibrium spectrum)

$$S(\omega) = \frac{4\gamma_0 k_B T}{N} \sum_{q=0}^{N-1} \frac{1 - \cos(2\pi q/N)}{[r_1^2(q) + \omega^2][r_2^2(q) + \omega^2]} \quad (14)$$

where

$$r_{1,2}(q) = -\frac{\gamma_0}{2} \pm \sqrt{\left(\frac{\gamma_0}{2}\right)^2 - 4k \sin^2\left(\frac{\pi q}{N}\right)}. \quad (15)$$

In two dimensions

$$S(\omega) = \frac{4\gamma_0 k_B T}{N^2} \sum_{p,q=0}^{N-1} \frac{2 - \cos(2\pi p/N) - \cos(2\pi q/N)}{[r_1^2(p, q) + \omega^2][r_2^2(p, q) + \omega^2]} \quad (16)$$

where now

$$r_{1,2}(p, q) = -\frac{\gamma_0}{2} \pm \sqrt{\left(\frac{\gamma_0}{2}\right)^2 - 4k \left[\sin^2\left(\frac{\pi p}{N}\right) + \sin^2\left(\frac{\pi q}{N}\right) \right]}. \quad (17)$$

For anharmonic chains these spectra must be obtained numerically.

To monitor the decay of the spectrum when the thermalized arrays are connected to a cold reservoir we introduce the time-dependent spectra

$$S(\omega, t) \equiv 2 \int_0^{\tau_{max}} d\tau C(\tau, t) \cos \omega \tau \quad (18)$$

where $\tau_{max} \equiv 2\pi/\omega_{min}$ and ω_{min} is chosen for a desired frequency resolution; the choice $\omega_{min} = 0.0982$, corresponding to $\tau_{max} = 64$, turns out to be numerically convenient. The time-dependent correlation function is actually an average over the time interval $t - t_0$ to t , where we have chosen $t_0 = 100$ (short enough for the correlation function not to change appreciably but long enough for statistical purposes) and is defined as follows in one dimension:

$$C(\tau, t) = \frac{1}{(N-1)} \sum_{i=2}^N \frac{1}{\Delta t} \int_0^{\Delta t} d\tau' \langle \delta_i x_i(t - \tau') \delta_i x_i(t - \tau' - \tau) \rangle, \quad (19)$$

where $\Delta t \equiv t_0 - \tau_{max}$. The generalization to the two-dimensional case is obvious.

3 Thermal Relaxation

We start by presenting two sets of figures, each associated with one of the measures for relaxation mentioned in the previous section. Each set presents

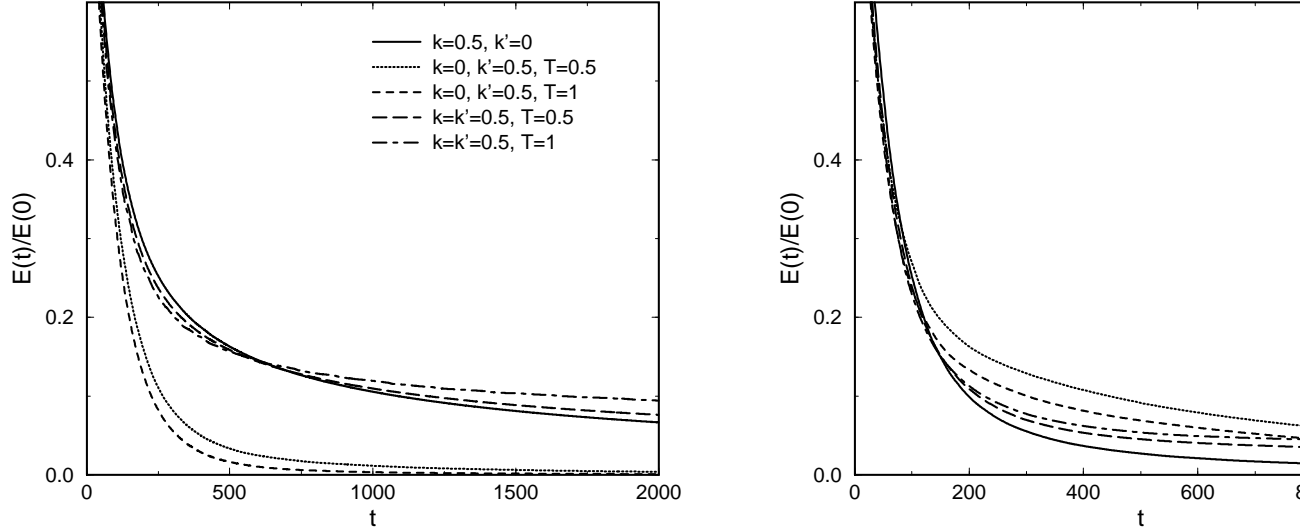


Figure 1: Temporal relaxation of the fractional energy for different arrays with potential parameters and initial temperatures indicated in the panels. First panel: one dimension ($N = 50$). Second panel: two dimensions (20×20 lattices). In all cases $\gamma = 0.1$. The fractional energy for the harmonic arrays is independent of temperature.

both 1d and 2d results. Along with these results we present some auxiliary figures that help in the interpretation of the outcomes.

The total energy of a relaxing array decays in time, and the questions of interest are how exactly the energy decreases with time for arrays with different interactions and in different dimensions. The answers are illustrated in Fig. 1. Accompanying these decay curves are the more detailed spectral decay curves shown in Fig. 2.

The decay of the total energy ratio for harmonic systems is independent of temperature, which is verified numerically and therefore leads to a single curve in Fig. 1 in each dimension for the given parameters k , N , and γ . The initial exponential decay of the energy in both one and two dimensions, and the N and γ dependences of the decay rate, have been verified numerically. The long-time decay as an inverse power law $E(t)/E(0) \sim t^{-\alpha}$ for both cases

has also been verified. It is interesting to note that Eq. (5) can be rewritten as an integral that makes explicit the cascade of relaxation times giving rise to the inverse power law behavior:

$$\frac{E(t)}{E(0)} = e^{-t/\tau_0} I_0(t/\tau_0) = \frac{\sqrt{\tau_0/2}}{\pi} \int_{\tau_0/2}^{\infty} d\tau \frac{e^{-t/\tau}}{\tau \sqrt{\tau - \tau_0/2}}. \quad (20)$$

The lower limit, due to a nonzero shortest decay time, leads to the initial exponential decay of the energy, but it is the long $\tau^{-3/2}$ tail of slow relaxation times that leads to the power law decay. We return to this point below.

The associated spectra for the harmonic arrays are shown in each of the first frames of the two panels in Fig. 2. The evolution confirms that *low* frequencies decay more rapidly in the harmonic chain – the spectrum is absorbed by the cold reservoir from the bottom up, and by the latest times shown, only the longer-lived band-edge modes remain in the system. Since each spectral component is associated with an independent phonon, the spectral decrease occurs “vertically”, that is, each spectral component decays directly into the reservoir on its characteristic time scale; this is shown schematically for the one-dimensional systems in Fig. 3, where the downward arrows represent absorption by the reservoir and their relative length schematizes the absorption rate.

For anharmonic arrays the relaxation behavior depends strongly on the presence or absence of a harmonic component in the potential, and, in some respects, on dimensionality. First we consider the purely anharmonic arrays. The dimensionality plays a particularly important role in this case.

In one dimension the upper panel of Fig. 1 shows an essentially purely exponential decay (verified separately), which is characteristic of a single predominant decay channel. The decay is more rapid at higher temperatures. Note that there are no phonons in this purely quartic system, so that single frequencies are not associated with normal modes of the system. Conversely, exact solutions of the FPU chain such as solitons and intrinsic localized modes may involve many frequencies. The second frame in the upper panel of Fig. 2 shows that the higher frequencies decay first, exactly opposite to the harmonic chain. We find that the relaxation pathway is for the high frequency portions of the spectrum to degrade rapidly into lower frequency excitations, as schematically indicated by the sloped arrows in Fig. 3. The lowest frequencies decay into the reservoir and define the exponential decay rate seen in Fig. 1. In more detail, the high frequency components of the spectrum are

mainly due to highly mobile localized modes that degrade into lower energy (less mobile) excitations as they move and collide with one another. The lowest frequency excitations are in turn absorbed into the cold reservoir but continue to be replenished through the degradation process. It is important to note, however, that among the low frequency excitations are some that persist for a very long time, certainly beyond the times of our simulations. Their decay is surely slower than exponential, perhaps a stretched exponential. These, the only remaining spectral components at time $t = 2000$, are “labeled” by short downward arrows in the relaxation schematic and include rather stable breather and/or soliton modes that move very slowly and are localized away from the boundaries. Also, some direct relaxation of all frequency components into the reservoir occurs as well (shown schematically by the short arrows at high frequencies in Fig. 3), but this direct relaxation is slower than the energy degradation pathway. For example, when a highly mobile localized excitation reaches a boundary, it typically remains at the boundary for about one period of oscillation (which is short for a highly energetic excitation), during which it loses a small portion of its energy to the reservoir. The remaining excitation is reflected back into the chain, where it will continue to lose energy through other collision events and/or re-arrival at the boundaries. The role of high-frequency mobile modes and of low-frequency slowly moving or stationary modes in this picture will be tested in more detail in the next section, where we explicitly inject a high-frequency localized mode into the array and observe the relaxation dynamics. We do note here that our picture is consistent with known facts about localized states. In particular, it is known that higher-frequency and/or higher amplitude localized modes can move at higher velocities [9, 12, 16]. It is also known that while in motion such modes lose energy through collisions with other excitations. Figure 1 shows a faster decay at higher temperatures, which is consistent with our observations elsewhere that the speed of an injected pulse (and therefore, we conjecture, the speed of a moving localized mode) in these arrays increases with temperature [13].

The relaxation dynamics of the purely anharmonic array in two dimensions differs from the one-dimensional case in a number of ways. First, we note that the decay of the energy in Fig. 1 is (except for very early times) slower in the hard array than in the harmonic one over the times of observation. Second, except for an initial short time interval, the decay is found not to be exponential, indicating that there is no longer a single predominant decay channel as there was in one dimension. In two dimensions the relax-

ation pathway again includes degradation of higher frequency excitations to lower frequencies, as can be seen in the spectral rendition in Fig. 2. However, whereas in one dimension the degradation process is faster than the decay of low frequency excitations into the reservoir (and hence this latter decay is the rate-limiting step that defines the total energy decay process), here the degradation process is slower, leading to spectral bottlenecks and competing time scales. We find that increasing the array size leads to slower degradation of the high frequency components and to more pronounced spectral bottlenecks in the mid-frequency range. Our physical picture of the source of the competing time scales involves the observation that in two dimensions, localized excitations are not nearly as mobile as in one dimension. In one dimension energy degradation occurs as a consequence of high mobility and the resultant inevitable frequent scattering. The reduced mobility in two dimensions was noted in earlier work on pulse propagation [13] and will be supported and clarified in the next section, where we explicitly inject a high-amplitude breather into our system. At long times in the 2d system excitations of all energies eventually reach the boundaries. These excitations typically lose some of their energy into the cold reservoir and the remainder is reflected back into the array, where it either degrades into lower energy components or reaches a boundary again with the attendant energy loss. Note also that with increasing temperature the total system energy decays more rapidly, which is consistent with our assertion that mobility (low as it may be) in the purely hard arrays increases with temperature because of the participation of more mobile higher frequency components in the initial equilibrium mix of excitations.

The result is an energy decay that is of stretched exponential form,

$$\frac{E(t)}{E(0)} \sim e^{-(t/\tau)^\sigma}, \quad (21)$$

as is evident in the first panel of Fig. 4, where we plot

$$\beta(t) = \frac{d}{d \ln t} \ln \left[-\ln \left(\frac{E(t)}{E(0)} \right) \right] \quad (22)$$

as a function of time for four purely anharmonic 2d arrays of different sizes, damping coefficients, and temperatures. When the decay is a stretched exponential this rendition gives a flat line at the value $\beta(t) = \sigma$. We find that the value of σ is independent of temperature, as seen in the figure (we have

tested this assertion for various lattice sizes in the range $T = 0.1 - 1.0$), and that it increases with γ , as also seen in the figure. For the 20×20 lattices we find that σ is around 0.33 for $\gamma = 0.1$ and $\sigma \approx 0.43$ for $\gamma = 1$. The temperature independence is explained by the fact that temperature does not dominate the mobility of the residual excitations nor does it determine their rate of energy loss once they reach a boundary. On the other hand, it is reasonable that increasing γ leads to a faster long-time relaxation process (larger σ) because more energy is lost to the reservoir upon each collision. We find that σ also increases with N , which is somewhat of a puzzle. We find, for instance, that in a 50×50 array with $\gamma = 0.1$ (and for any temperature) $\sigma \approx 0.52$. The issue of the size dependence of relaxational processes following a stretched exponential behavior is a difficult problem that has only recently been addressed in a different context [23]. In summary, for the purely anharmonic 2d arrays

$$\sigma = \sigma(N, \gamma). \quad (23)$$

The mixed arrays, i.e., those with interactions that have both quadratic and quartic potential contributions, are of course the ubiquitous FPU systems since it is difficult to envision a “real” physical system that has no quadratic potential terms (one might also say this about cubic potential terms that have not been included here [24]). The thermal relaxation of these arrays proceeds similarly in one and two dimensions. At early and intermediate times the mixed arrays relax very similarly to the harmonic arrays (i.e., exponential decay followed by power law decay), albeit somewhat modified and speeded up by the presence of high-frequency mobile excitations in addition to the low-frequency phononic excitations. The rapid decay of both low and high frequency excitations is evident in the third frames of both panels in Fig. 2. This similarity in one dimension was noted by Piazza et al. [10]. After some time, however, the mixed chain relaxation behavior changes to a stretched exponential. This occurs when the low frequency modes have essentially all decayed. The higher frequency spectral components that persist are localized long-lived excitations (note that high-frequency phonon modes are unstable against breather formation in these systems [12]). Unlike the purely anharmonic array, here there is no low-frequency residue to perturb the high-frequency localized excitations and so they survive relatively unperturbed and immobile for a long time. The persistence of high-frequency spectral components is seen in the third frames of both panels in Fig. 2, and the schematic representation of the progression in one dimension is shown

in Fig. 3. The slow leakage of breather energy into low energy modes that continue to dissipate into the cold reservoir is responsible for the eventual stretched exponential relaxation of the system.

These behaviors can be seen clearly in the second panel of Fig. 4 which shows $\beta(t)$ for various 1d and 2d mixed arrays. The initial exponential behavior (which corresponds to a flat curve at $\beta(t) = 1$), occurs over too short a time scale to be clearly discernible. There then follows a power law decay regime which eventually turns to a stretched exponential. In the power law regime, if the energy decays as $E(t)/E(0) \sim (t/\tau_0)^{-\alpha}$ then it follows that $\beta(t) = \left(\ln \frac{t}{\tau_0}\right)^{-1}$, which is independent of α and depends only on the ratio N/γ via τ_0 . The two 2d curves and the 1d curve with the same value of N/γ are all seen to decay with the same slope. As all the curves settle into their asymptotic behavior, we see that σ depends neither on N nor on γ : the two 1d arrays are of different sizes but asymptote to the same σ (approximately 0.21), as do the two 2d arrays of the same size and initial temperature but with different damping coefficients ($\sigma \approx 0.03$). On the other hand, the 2d arrays that have different initial temperatures asymptote to different values of σ (approximately 0.25 for $T = 0.1$ and around 0.03 for $T = 0.5$). The observed behavior is explained by the fact that the slow leakage of energy out of the long-lived localized excitations is rate limiting. A higher initial temperature leads to more energetic, more stable breathers with slower leakage, hence explaining why σ decreases with increasing temperature. Neither the size of the system nor the damping coefficient are important in this limit, since the slowest process is the leakage. The low-energy outcome of that leakage is absorbed quickly by the cold reservoir. Note that this description is consistent with that provided for relaxation of lattices with local anharmonic potentials [22]. In summary, for 1d and 2d arrays with quadratic plus quartic interaction potentials

$$\sigma = \sigma(T). \quad (24)$$

It is interesting to stress that, like an inverse power law decay, a stretched exponential can indeed be obtained from a distribution or hierarchical progression of decay times. For example,

$$e^{-(t/\tau_1)^{1/2}} = \frac{1}{2\sqrt{\pi\tau_1}} \int_0^\infty d\tau e^{-t/\tau} \frac{e^{-\tau/4\tau_1}}{\tau^{1/2}}, \quad (25)$$

which should be compared with Eq. (20). More generally, if the distribution of relaxation times varies as $e^{-(\tau/\tau_1)^\mu}$, then the decay will go as a stretched exponential with $\sigma \sim 1/(1 + \mu)$ at long times (the stretched exponential with $\sigma = 1/2$ is the only one whose associated distribution is expressible in extremely simple analytic form, but distributions associated with other fractional exponents are also known analytically or numerically [25]). The distributions leading to inverse power decay and to a stretched exponential decay are both broad, but the inverse power law of course arises explicitly from very long tails not present in the stretched exponential. In other words, the relaxation of the last energy residues of a very large harmonic lattice take *longer* than those of a very large anharmonic lattice. There is an important difference, however: in the harmonic lattice the persistent excitations are distributed over the entire lattice, while in the anharmonic lattice they are localized. Also, in a *finite* lattice eventually the harmonic decay is again exponential while that of the anharmonic system remains a stretched exponential.

Spatial energy landscapes rendered in gray scale provide a pictorial representation of the thermalization progressions. We follow widespread convention and define the local energy in one dimension as

$$E_i = \frac{\dot{x}_i^2}{2} + \frac{1}{2} [V(x_i - x_{i-1}) + V(x_{i+1} - x_i)] \quad (26)$$

with obvious generalization in two dimensions. Figure 5 shows the temporal evolution of the local energy landscape for each of the three chains. Particularly dramatic is the spontaneous occurrence of an essentially stationary breather in the mixed chain. It is this sort of breather that leads to the extremely slow relaxation of the mixed chain energy. Spatial landscapes for two-dimensional systems are shown in six time frames in Figs. 6 and 7 for the pure anharmonic and the mixed anharmonic lattices, respectively. Note that in the purely hard array the localized high-energy regions move around and relax within the time scale of the progression. In the mixed array, on the other hand, the “hot spots” persist and essentially do not move.

4 Relaxation With an Injected Breather

Our portrayal of the thermal relaxation process can be further bolstered by initially injecting a high-energy localized excitation in the center of each

thermalized array and observing the behavior of this excitation during the relaxation process. Some of the dimensionality differences are thereby clarified. The injected excitation is chosen so as to be close to a known exact breather solution of the anharmonic arrays.

In a one-dimensional array with an interaction potential $V(x_i - x_{i-1}) = (x_i - x_{i-1})^n$ as $n \rightarrow \infty$ and exact odd-parity breather is one of amplitude A at a site and $-A/2$ at each of the two immediately adjacent sites. An exact even-parity breather is one with amplitude A at one site and $-A$ at an immediately adjacent site. These are not exact solutions when n is not infinite and/or when there are quadratic contributions to the potential, but they are close to exact, even for the FPU chain [26, 27]. In two dimensions the odd-parity solution with amplitude A at one site and amplitudes $-A/4$ at the four nearest neighboring sites is also nearly exact, but there is no equivalent to the even-parity breather. We insert an odd-parity excitation at the center of our array and in each case choose arrays sufficiently large (300 sites in one dimension, 30×30 in two dimensions) so that the excitation either decays or stops moving before ever reaching the boundaries. In harmonic arrays the fate of such an injected excitation is completely predictable and uninteresting: it spreads quickly over the entire array and thus loses its localized character. The associated Fourier decomposition into phonon modes dictates the relaxation behavior.

To follow the excitation in the one-dimensional anharmonic arrays we calculate the mean squared displacement

$$\langle x^2(t) \rangle \equiv \left\langle \left(i_{max}(t) - \frac{N}{2} \right)^2 \right\rangle \quad (27)$$

as a measure of the position of the excitation (its dispersion in the anharmonic chains is very small [13]). Here $N/2$ is the initial point of highest energy in the chain and $i_{max}(t)$ is the point of maximum energy at time t . Similarly, in two dimensions we define

$$\langle r^2(t) \rangle \equiv \left\langle \left(i_{x,max}(t) - \frac{N}{2} \right)^2 \right\rangle + \left\langle \left(i_{y,max}(t) - \frac{N}{2} \right)^2 \right\rangle \quad (28)$$

where $(N/2, N/2)$ is the initial point of highest energy and $(i_{x,max}(t), i_{y,max}(t))$ is the point of maximum energy at time t .

In a purely anharmonic chain in one dimension, a short time after it is created the excitation begins to move essentially ballistically in one direction

or the other with equal probability. The motion continues for a period of random duration, until the excitation stops moving for a random period of time. Then it moves again in either direction. Whatever its initial parity, while subsequently stationary the excitation has even parity (the more stable of the two configurations). Any perturbation (usually scattering of slow low-frequency excitations) that disturbs this parity sets the breather in motion, and while it moves it alternates between even and odd parity. The excitation only loses energy while in motion, through collisions with persistent low-frequency excitations.

A typical mean squared displacement for the one-dimensional purely anharmonic array is shown in Fig. 8. The mean square displacement follows the superdiffusive law $\langle x^2(t) \rangle \sim t^\alpha$ with $\alpha = 1.5$ over the entire lifetime of the excitation. This particular exponent is recovered for the purely quartic chain under all conditions that we have tested, that is, independently of force constant, excitation amplitude, and temperature. Parameter variations affect only the prefactor, which reflects the breather velocity. Indeed, it does not matter *when* in the course of the relaxation process the localized excitation is introduced: its mean squared displacement grows with the same exponent 1.5 until the excitation is extinguished into the background. This confirms the role of the persistent low-frequency excitations. We have argued [20] that this particular superdiffusive exponent can be understood in terms of scattering events that occur with a time distribution $\nu(t) \sim t^{-5/2}$ [28].

In a purely anharmonic two-dimensional array the motion is rather different (which is consistent with the spectral differences in one and two dimensions). A typical mean squared displacement is also shown in Fig. 8. The law is now sub diffusive, $\langle r^2(t) \rangle \sim t^\alpha$ with $\alpha = 0.89$ over the lifetime of the excitation. Again, this exponent is insensitive to force constant, excitation amplitude, and temperature changes. It does reflect the fact that the excitation moves much less in two dimensions than in one (although it does of course move and eventually recedes into the background). In earlier work [13] we noted that a pulse in a one dimensional purely hard array tends to move more rapidly but remains more tightly concentrated than a pulse in, say, a harmonic or soft array. We also noted that in two (or more) dimensions these two tendencies are in some sense contradictory since the only way that a symmetric excitation can move is by breaking its symmetry and/or dispersing. The sort of perturbation that would set a breather in motion requires an asymmetry that is more difficult to achieve in two dimensions than in one. If the distribution of collision times of energetic breathers

with other excitations that can set it in motion has sufficiently long quiescent periods (long-tailed waiting time probability distribution function) then the motion of the excitations is typically subdiffusive [29]. Note that this does not preclude collisions that lead to energy loss by the breather even if it is not set in motion.

The situation in mixed anharmonic arrays is similar in one and two dimensions, see Fig. 8. The injected excitations at first move with the same characteristic exponents α as in the corresponding purely anharmonic systems, but as the harmonic interactions sweep the background thermal energy out of the system, the localized excitations stop moving. The mean squared displacement in each dimension then becomes independent of time (earlier in two dimensions than in one).

5 Summary

Energy relaxation in one- and two-dimensional nonlinear arrays with quartic interparticle interactions (Fermi-Pasta-Ulam or FPU arrays) proceeds along energetic pathways completely different from those of harmonic systems and is quite sensitive to the presence or absence of quadratic contributions to the interactions. Relaxation in a purely harmonic array involves the sequential decay of independent phonon modes starting with those of lowest frequency and moving upward across the spectrum. The decay of energy in these arrays is exponential at short and long times, but follows an inverse power law at intermediate times. Throughout the decay process, the energy is distributed uniformly over the entire array. A localized excitation injected in the lattice simply decays according to the distribution of characteristic relaxation times of its phonon components.

FPU arrays with quadratic and quartic interactions contain phonon-like modes as well as high-energy nonlinear, and to varying degrees localized, excitations (provided the initial temperature is sufficiently high to excite these). The relaxation process involves the decay of phonons in the same spectral order as in the harmonic arrays and also energy losses through collisions of mobile high-energy localized excitations as they collide with lower-frequency ones. Eventually the harmonic interactions succeed in “sweeping” the system clean of low energy excitations and the remaining localized modes are quasistationary breather solutions that persist for a very long time. The decay to this quasistationary state is a stretched exponential with an exponent that

depends on temperature but not on system size or damping coefficient. An explicitly injected high-energy localized breather follows this behavior, with a mean squared displacement that at first grows with time but then becomes independent of time when the system has been swept clean of background excitations.

The greatest differences between one- and two-dimensional FPU arrays occur in the purely quartic arrays. In all cases the relaxation begins from the high-frequency end of the spectrum (opposite to the harmonic case) and involves not a direct absorption by the cold reservoir but rather a degradation of high-frequency excitations to lower-frequency ones. In one dimension this degradation process is considerably faster than in two dimensions. The lowest frequency modes in one dimension are absorbed by the cold reservoir but are quickly replenished by the degradation process. The energy relaxation is essentially exponential, with a time constant determined by the decay of the lowest frequency components. In two dimensions the degradation process is slower and there are frequency bottlenecks so that the decay of the lowest frequency excitations into the cold reservoir no longer constitutes the rate limiting process. Instead, the degradation and decay contribute to a resulting stretched exponential energy decay with an exponent that depends on system size and damping coefficient but is independent of temperature. In both one and two dimensions there remains a thermal residue of localized low-frequency excitations that continue to perturb and degrade higher frequency ones. The array is never “swept clean” of low-energy excitations as is the mixed array, and therefore no persistent breathers occur in this system. In order to confirm this behavior we have followed the dynamics of an injected high-frequency localized excitation in these arrays. In one dimension this localized excitation remains localized but is very mobile throughout its lifetime, being characterized by a super-diffusive mean squared displacement. In two dimensions the excitation also remains localized and is much less mobile (but nevertheless, always mobile until it disappears), being characterized by sub-diffusive motion.

Acknowledgments

This work was supported in part by the Engineering Research Program of the Office of Basic Energy Sciences at the U. S. Department of Energy under Grant No. DE-FG03-86ER13606. Partial support was provided by a grant

from the University of California Institute for México and the United States (UC MEXUS) and the Consejo Nacional de Ciencia y Tecnología de México (CONACYT), and by IGPP under project Los Alamos/DOE 822AR.

References

- [1] M. Peyrard and J. Farago, *Physica A* **288**, 199 (2000).
- [2] G. Kopidakis and S. Aubry, *Physica B* **296**, 237 (2001).
- [3] H. Berg, *Nature* **394**, 324 (1998).
- [4] W. O. Hancock and J. Howard, *J. Cell Biol.* **140**, 1395 (1998).
- [5] A. Xie, L. Van der Meer, W. Hoff and R.H. Austin, *Phys. Rev. Lett.* **84**, 5435 (2000).
- [6] T. Rössler and J. B. Page, *Phys. Rev. B* **62**, 11460 (2000).
- [7] S. F. Mingaleev, Y. S. Kivshar and R. A. Sammut, *Phys. Rev. E* **62**, 5777 (2000).
- [8] S. Aubry and K. Kopidakis, *cond-mat/0102162*.
- [9] R. Bourbonnais and R. Maynard, *Int. J. of Mod. Phys. C* **1**, 233 (1990).
- [10] F. Piazza, S. Lepri, and R. Livi, *nlin.CD/0105028*.
- [11] R. Reigada, A. Sarmiento, A. H. Romero, J. M. Sancho and K. Lindenberg, *J. Chem. Phys.* **112**, 10615 (2000).
- [12] T. Cretegy, T. Dauxois, S. Ruffo and A. Torcini, *Physica D* **121**, 109 (1998).
- [13] A. Sarmiento, R. Reigada, A. H. Romero and K. Lindenberg, *Phys. Rev. E* **60**, 5317 (1999).
- [14] R. Reigada, A. Sarmiento and K. Lindenberg, *Phys. Rev. E* **63**, 066113 (2001).
- [15] V. M. Burlakov, S. A. Kiselev, and V. N. Prykov, *Phys. Rev. B* **42**, 4921 (1990).

- [16] Y. A. Kosevich and S. Lepri, Phys. Rev. B **61**, 299 (2000).
- [17] J. L. Marín, F. Falo, P. J. Martínez and L. M. Floría, nlin.PS/0103013.
- [18] S. Flach and C. R. Willis, Physics Reports **295**, 181 (1998).
- [19] S. Aubry, Physica D **103**, 201 (1997).
- [20] R. Reigada, A. Sarmiento and K. Lindenberg, cond-mat/0108148, to appear in Phys. Rev. E.
- [21] G. P. Tsironis and S. Aubry, Phys. Rev. Lett. **77**, 5225 (1996).
- [22] A. Bikaki, N. K. Voulgarakis, S. Aubry and G. P. Tsironis, Phys. Rev. E. **59**, 1234 (1999).
- [23] A. Bunde, S. Havlin, J. Klafter, G. Gräff and A. Shehter, Phys. Rev. Lett. **78**, 3338 (1997).
- [24] R. Reigada, A. Sarmiento and K. Lindenberg, in preparation.
- [25] E. W. Montroll and J. T. Bendler, J. Stat. Phys. **34**, 129 (1984).
- [26] S. Flach, Phys. Rev. E **51**, 1503 (1995).
- [27] J. L. Marin, S. Aubry, Nonlinearity **9**, 1501 (1996).
- [28] E. Barkai, V. Fleurov and J. Klafter, Phys. Rev. E **61**, 1164 (2000).
- [29] R. Metzler and J. Klafter, Phys. Rep. **339**, 1 (2000).

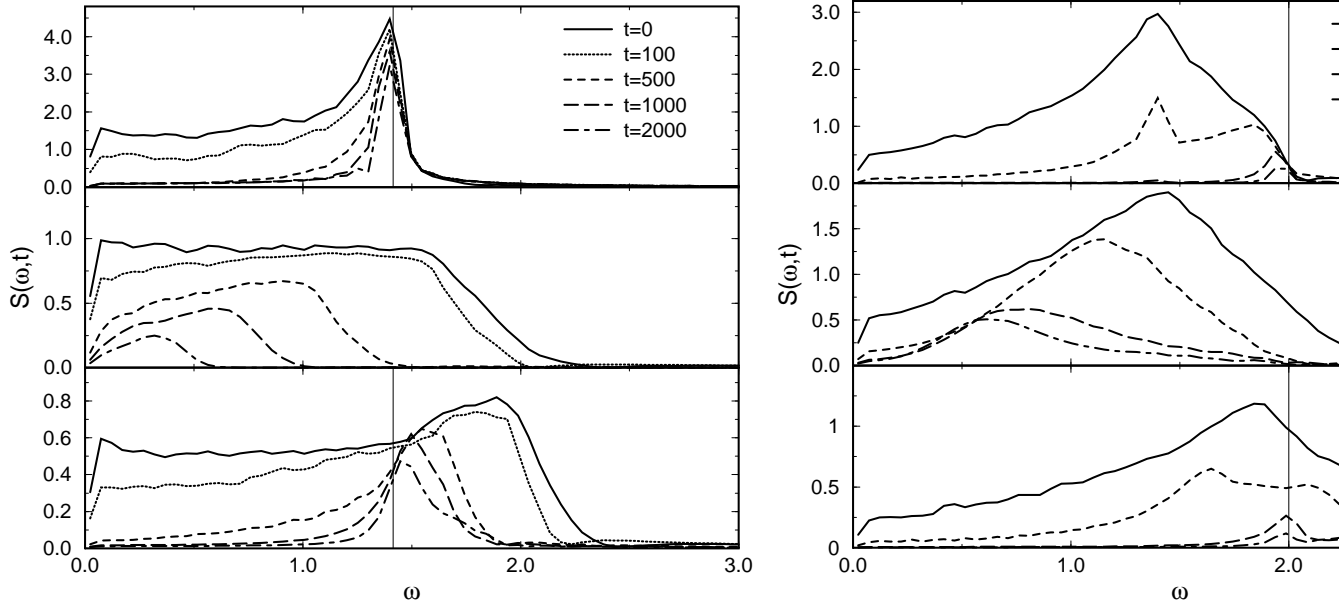


Figure 2: Time evolution of spectra for various relaxing arrays. The upper three-frame panel is for one-dimensional (50 sites) arrays, the lower three-frame panel for two-dimensional (20×20 sites) arrays. First frames: harmonic interactions ($k = 0.5$). Second frames: purely anharmonic interactions ($k' = 0.5$). Third frames: mixed interactions ($k = k' = 0.5$). The time progression is as indicated. The $t = 0$ spectrum (solid curves) in each case is the equilibrium spectrum at $T = 0.5$, the initial temperature. In all cases $\gamma = 0.1$. The thin vertical lines indicate the frequencies $\omega = \sqrt{4k} = \sqrt{2}$ (1d panels) and $\omega = 2$ (2d panels).

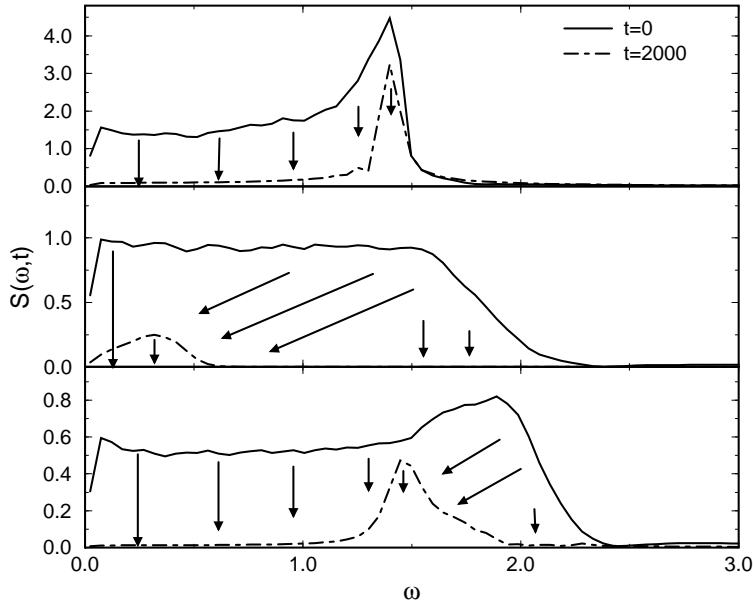


Figure 3: Schematic representation of the spectral relaxation channels in one dimension. The one-dimensional spectra of Fig. 2 for times $t = 0$ and $t = 2000$ are shown again here, and the arrows depict the pathways of different spectral components. Downward arrows indicate absorption by the cold reservoir, while angled arrows denote degradation from one spectral region to another. The relative lengths of the arrows depict the associated rates.

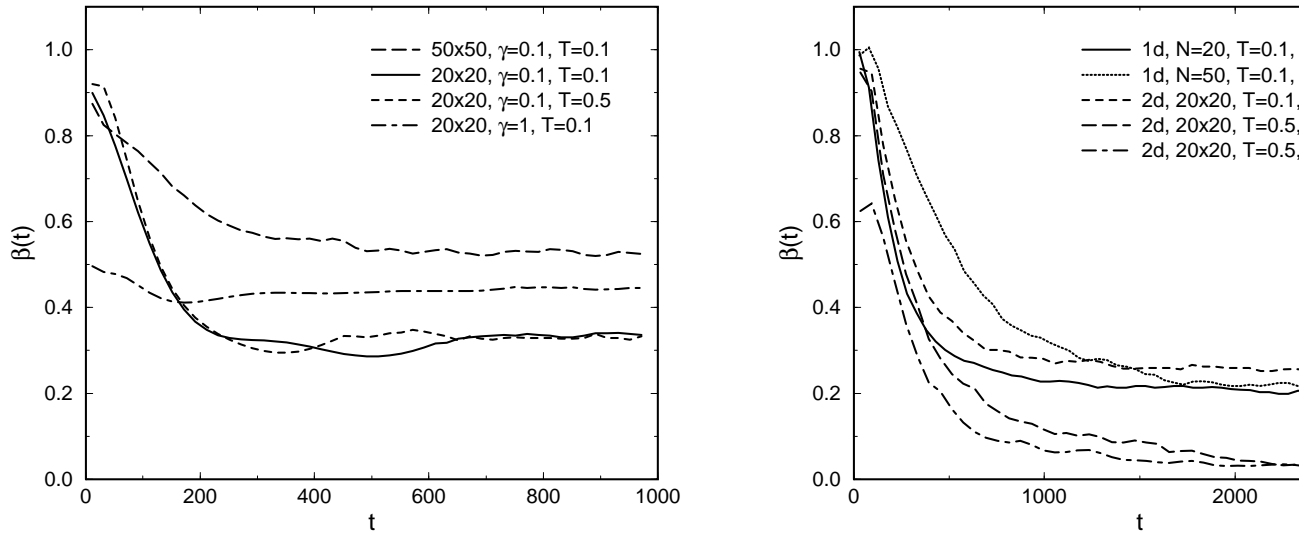


Figure 4: Plot of $\beta(t)$ as a function of time. A flat line below $\beta(t) = 1$ indicates stretched exponential behavior. First panel: purely anharmonic 2d arrays of different sizes, damping coefficients, and temperatures. Second panel: various 1d and 2d mixed arrays.

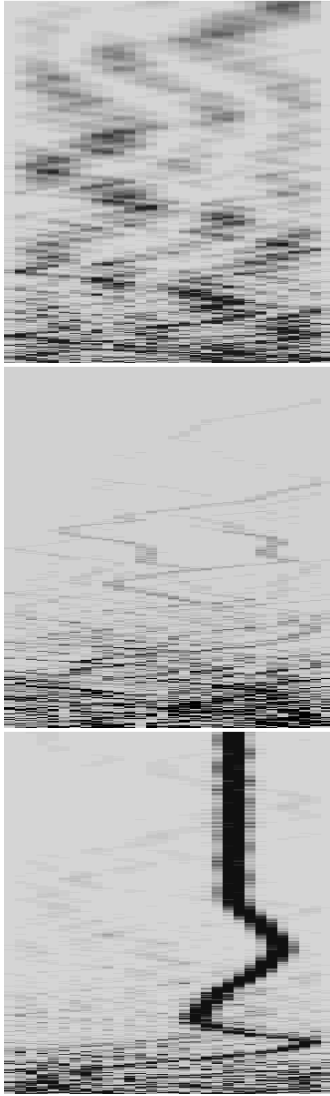


Figure 5: Local energy landscapes of one-dimensional 30-site arrays initially thermalized at $T = 0.5$. Time advances along the y -axis until $t = 1000$. A gray scale is used to represent the local energy, with darker shading corresponding to more energetic regions. First panel: harmonic chain, $k = 0.5$ and $k' = 0$. Second panel: purely anharmonic chain, $k = 0$ and $k' = 0.5$. Third panel: mixed chain, $k = k' = 0.5$.

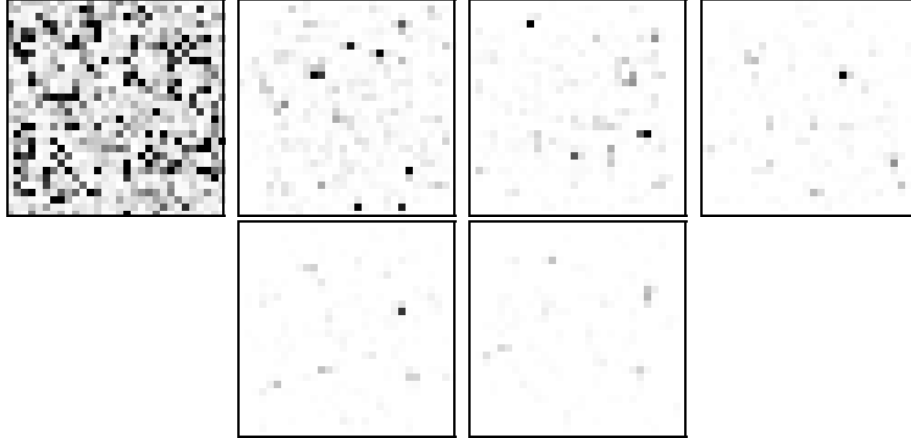


Figure 6: Local energy landscapes for a 20×20 purely anharmonic lattice ($k' = 0.5$) initially thermalized at $T = 0.5$ and with $\gamma = 0.1$. From first to last frames: $t = 0, 400, 800, 1200, 1600,$ and 2000 .

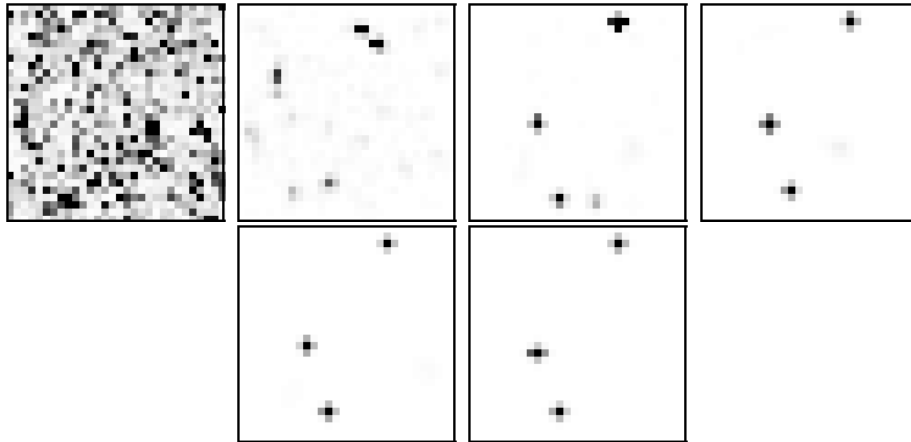


Figure 7: Local energy landscapes for a 20×20 mixed anharmonic lattice ($k = k' = 0.5$) initially thermalized at $T = 0.5$ and with $\gamma = 0.1$. From first to last frames: $t = 0, 400, 800, 1200, 1600,$ and 2000 .

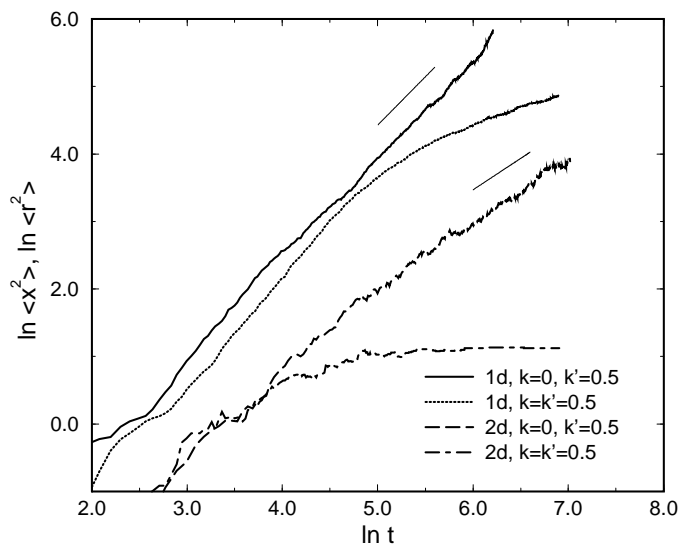


Figure 8: Mean squared displacement of a localized mode in various one dimensional (300 sites) and two dimensional (30×30) FPU arrays. The slopes of the two short straight lines are 1.5 and 0.89. In all cases $A = 2$, $T = 0.1$, and $\gamma = 0.1$.